Electrochemical and Adsorption Study of the anticorrosion behavior of Cefepime on Pipeline steel surface in acidic Solution

N. B. Iroha[1*], L. A. Nnanna[2]

[1]*Electrochemistry and Material Science Unit, Department of Chemistry, Federal University, Otuoke, Bayelsa, Nigeria.*
[2]*Department of Physics, Michael Okpara University of Agriculture, Umudike, Abia State, Nigeria.*

Abstract

The anticorrosion behavior of cefepime, a fourth-generation cephalosporin antibiotic, in controlling X80 pipeline steel corrosion in 1.0 M HCl solution was investigated by weight loss and electrochemical methods. The acid corrosion of the pipeline steel was inhibited in the presence cefepime which formed a protective layer on the steel surface by adsorption. Increase in cefepime concentration improved its adsorption on the steel surface and increased the inhibition efficiency. Electrochemical impedance spectroscopy (EIS) results revealed that charge transfer resistance increased as concentration of cefepime increases, which indicate adsorption of the inhibitor species on the steel surface. The results of potentiodynamic polarization (PDP) revealed that cefepime behaved as a mixed type inhibitor but showed the predomination of anodic reaction inhibition. The adsorption of cefepime on X80 pipeline steel surface obeyed the Langmuir adsorption isotherm. Morphological analysis conducted by scanning electron microscopy (SEM) showed smoother steel surface in the presence of cefepime than without the inhibitor.
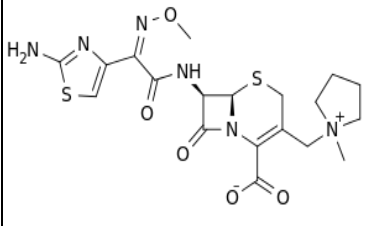
1. Introduction

The high strength of X80 steel has made it a choice material in oil-well processing equipment and for the construction of pipelines in the oil and gas industry. Oil-well acidizing is one of the practices in the petroleum industry for improving productivity (stimulation) of wells. Acidizing involves pumping acid into a wellbore or geologic formation that is capable of producing oil and/or gas, a process which normally leads to corrosion dissolution [1]. The corrosion reaction can be suppressed by the use of appropriate and effective acid corrosion inhibitors to protect the steel tubulars in the wells. Some organic compounds containing O, N, S heteroatoms in their moieties are known to be effective corrosion inhibitors for steel in acidic media [2-6]. The inhibitor molecules are adsorbed chemically or physically or both on the surface of the steel, hence forming a protective film on the steel surface that prevents corrosion [7].

The negative effect of most organic inhibitors on the environment has restricted their use in inhibiting metal corrosion. Nowadays, corrosion researchers are focusing on the exploration of environmentally safe corrosion inhibitors [8-12]. In the recent times, drugs have been used as corrosion inhibitors because they do not contain toxic species. Most drugs are actually synthesized from natural products of plant origin which puts them in a position to be classified as green corrosion inhibitors. There are many research work available which have reported the use of drugs as effective corrosion inhibitors for different metals in different corrosive media [13-16]. The inhibition mechanism of these drugs is ascribed to the blocking of the surface usually by formation of insoluble complexes on the surface of the metal.

Literature survey revealed that cefepime is a fourth-generation cephalosporin antibiotic which is non-toxic and has an extended spectrum of activity against gram-positive and gram-negative bacteria, with greater activity against both types of organism than third-generation cephalosporin. Cefepime is usually reserved to treat moderate to severe nosocomial pneumonia, infections caused by multiple drug-resistant microorganisms and empirical treatment of febrile neutropenia [17]. However, no report was found in literature on the use of cefepime as a corrosion inhibitor for any metal in acidic media. The structure, IUPAC name, molecular weight, molecular

formula and active centers of cefepime are shown in Table 1. The present work reports a study of the corrosion inhibitive effect of cefepime on X80 pipeline steel corrosion in 1 M HCl solution using weight loss, electrochemical impedance spectroscopy (EIS) and potentiodynamic polarization (PDP) techniques. Scanning electron microscopy (SEM) was used to perform the surface analysis of the steel.

Table 1: Structure, IUPAC name, molecular weight, molecular formula and active centers of Cefepime

Structure	IUPAC Name	Molecular weight	Active center	Chemical formula
	7-(2-(2-aminothiazol-4-yl)-2-(methoxyimino)acetamido)-3-((1-methylpyrrolidinium-1-yl)methyl)-8-oxo-5-thia-1-aza-bicyclo[4.2.0]oct-2-ene-2-carboxylate	480.56	5O 6N 2S	$C_{19}H_{24}N_6O_5S_2$

2. Material and Methods

2.1. Materials preparation

A flat sheet of X80 steel 5 mm in thickness with the following composition: C-0.065%, Si-0.24%, Mn-1.58%, P-0.011%, S-0.003%, Cu-0.01%, Cr-0.022%, Nb-0.057%, V-0.005%, Ti-0.024%, B-0.0006% and the balance is Fe was used for this study. The X80 steel sheet was obtained from Shell Nigeria oil field. The steel sheet was mechanically pressed-cut into coupons of dimension 1 cm × 1 cm for electrochemical measurements, 2 cm × 2 cm for gravimetric experiment and 2 cm × 1 cm for surface analysis examination. Before being used for the experiments, the X80 steel coupons were polished with 600 and 800 grades of emery paper, followed by cleaning with acetone, rinsing with distilled water, drying with air, weighing and used immediately. The blank corrodent was 1.0 M HCl solution prepared with distilled water.

Cefepime was purchased as Novapime, a brand manufactured by Lupin Limited, from Phillips Pharmaceuticals (Nig) Limited and used for the corrosion test. The inhibitor (Cefepime) was used as purchased without further purification or characterization. The inhibitor test solutions were prepared by dissolving earmarked mass of Cefepime in 1.0 M HCl solution in the concentrations range of 1 to 10 mM.

2.2. Weight loss studies

In this part of the experiment, the previously cleaned and weighed metal coupons were completely immersed in 1.0 M HCl solution in the absence and presence of different concentrations of Cefepime for 5 h maintained at 303 K in a thermostatic water bath. After immersion, the coupons were retrieved from their respective corroding test solutions, washed with 20% NaOH solution containing 4.0 g of Zinc dust to quench the corrosion reaction, rinsed in acetone, dried in warm air and reweighed [18]. The difference in weight of the coupons before and after immersion was taken as the weight loss. The experiments were repeated at temperatures of 313, 323 and 333 K respectively. All the tests were run in triplicate and the average value of the weight loss recorded. From the weight loss data, the corrosion rates (CR), degree of surface coverage (θ) and inhibition efficiency (%I_{WL}) were evaluated using Equations (1) – (3) respectively [19].

$$CR \ (mm/yr) = \frac{87.6 \ x \ \Delta w}{DAt} \qquad (1)$$

$$\theta = \frac{CR_{Ba} - CR_{In}}{CR_{Ba}} \qquad (2)$$

$$\%I_{WL} = 100(\theta) \qquad (3)$$

where ΔW is the average weight loss (mg), A is the cross sectional area of the coupon (cm²), t is the exposure time (h), D the density of the steel specimen (g cm⁻³), CR_{Ba} and CR_{Ih} are the corrosion rates (mm/yr) of steel in the blank acid and inhibited solutions respectively.

2.3. Electrochemical techniques

The electrochemical studies (PDP and EIS) were carried out using a CHI 660A electrochemical work station at 303 K. A three electrode cell assembly was used. The X80 pipeline steel prepared as shown in Section

2.1 with one face of the coupon of 1 cm^2 area exposed and the other face shielded with epoxy adhesives was the working electrode, saturated calomel electrode (SCE) was used as reference electrode and platinum electrode was used as the counter electrode (CE). Prior to the electrochemical measurement, the samples of X80 steel were first immersed in a blank solution for 30 minutes to establish a steady state open circuit potential (OCP). The potentiodynamic polarization study was performed from cathodic potential of -250 mV to anodic potential of +250 mV relative to corrosion potential at a scan rate of 0.2 mV/s. Impedance was measure with amplitude of 5 mV peak-to-peak in a frequency range of 100 kHz to 10 mHz using AC signals at respective corrosion potential (E$_{corr}$). Each experiment was run three times to check reproducibility and average values of the electrochemical data recorded. Data were analysed and curves fitted using Gamry E-Chem software. The linear Tafel region of the polarization curves were extrapolated to corrosion potential to obtain the corrosion current densities (I$_{corr}$). The charge transfers resistance (R$_{ct}$) values were obtained from the diameter of the semi circles of the Nyquist plots. Inhibition efficiency PDP (%I$_{PDP}$) and EIS (%I$_{EIS}$) was calculated for using Equations (4) and (5) respectively.

$$\%I_{PDP} = \left(1 - \frac{I_{corr(I)}}{I_{corr(B)}}\right)100 \qquad (4)$$

$$\%I_{EIS} = \left(\frac{R_{ct(I)} - R_{ct(B)}}{R_{ct(I)}}\right)100 \qquad (5)$$

where I$_{corr(I)}$ and I$_{corr(B)}$ are the measured corrosion current densities in the absence and presence of inhibitor respectively and R$_{ct(B)}$ and R$_{ct(I)}$ are measured charge transfer resistances in the absence and presence of inhibitor respectively.

2.4. Surface Morphological analysis

Morphological analysis of the X80 pipeline steel surface were done by SEM examinations of the steel surfaces using XL-30FEG Scanning electron microscope. X80 steel coupons were prepared as previously described in Section 2.1 and immersed for 5 h in 1.0 M HCl solution in the absence and presence of the 10 mM Cefepime at 303 K. The specimens were removed after immersion, washed with double distilled water, dried in acetone and mounted into the spectrometer for SEM examination [20].

3. Results and discussion

3.1. Weight loss studies

The plots of corrosion rate (CR) and inhibition efficiency (%I$_{WL}$) versus inhibitor concentration for X80 pipeline steel without and with different concentrations of Cefepime in 1.0 M HCl at different temperatures is shown in Figure 1 (a) and (b) respectively.
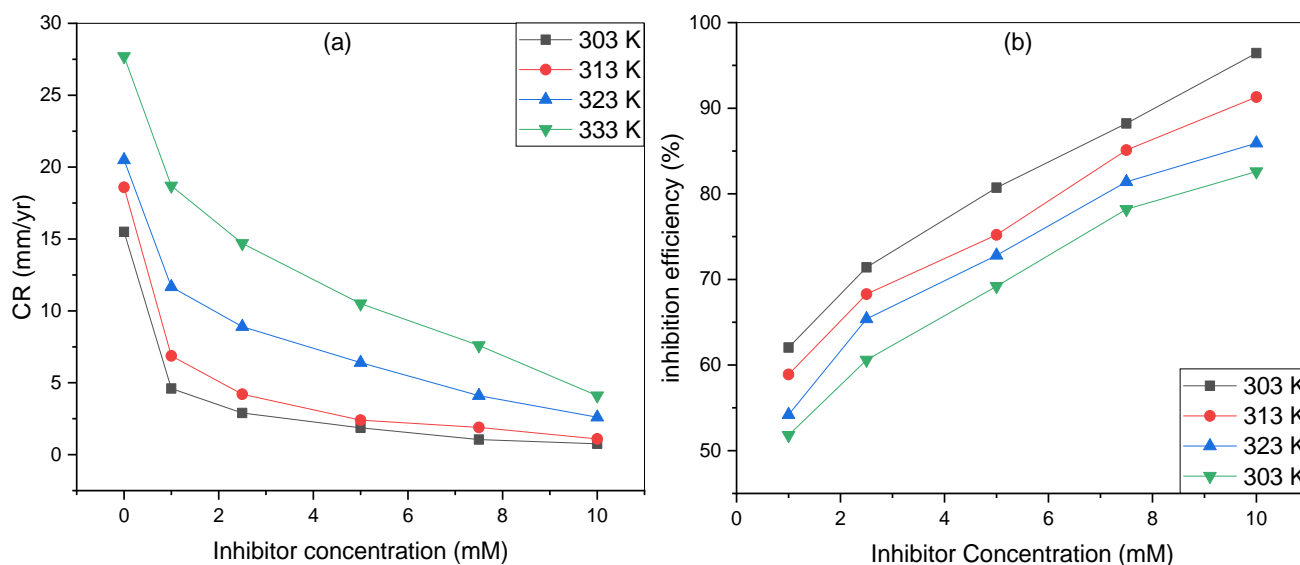

Figure 1: Variation of (a) corrosion rate and (b) inhibition efficiency (%I$_{WL}$) with Inhibitor concentration for X80 steel in 1 M HCl without and with different concentrations of Cefepime at different temperatures from weight loss measurements.

The result from Figure 1(a) reveals that CR of X80 steel reduced in the presence of Cefepime and the extent of reduction increased with increase in the concentration of the drug. This clearly indicates that Cefepime inhibited the corrosion of X80 steel in the acid solution. It was also noticed that the CR increased with increasing temperature from 303 to 333 K both in absence and presence of Cefepime. This is a pointer to the fact that the metal is susceptible to faster breakup with increase in thermal unrest of the corrosive environment. However, increase in the drug concentration increases %I_{WL}, but %I_{WL} decreases with increase in temperature (Figure 1b). The inhibition efficiency of Cefepime reached a maximum value of 96.4% at 303 K using 10 mM Cefepime which indicates that the X80 steel surface is efficiently separated from the acid solution by the adsorption of the inhibitor molecules on the steel surface [21, 22]. Decrease in %I_{WL} with increasing temperature may be due to desorption of the initially adsorbed molecules of the inhibitor or thermal degradation of Cefepime structure.

3.2. Adsorption isotherm

The corrosion inhibition ability of organic compounds is mainly due to adsorption onto a metal surface to form a protective film. A very important clue about the nature of the interaction between Cefepime and X80 pipeline steel surface can be provided by adsorption isotherms [23]. The process of adsorption of inhibitors is a displacement reaction, where the water molecules on the steel surface is replaced by the inhibitor molecules, expressed according to the equation:

$$Inh_{(sol)} + yH_2O_{(ads)} \rightarrow Inh_{(ads)} + yH_2O_{(sol)} \qquad (6)$$
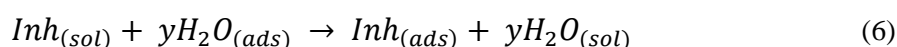
where $Inh_{(sol)}$ and $Inh_{(ads)}$ are the inhibitor added in the aqueous solution and adsorbed on the metal surface respectively, y is the number of adsorbed water molecules replaced by inhibitor molecule. The degree of surface coverage (θ) for different Cefepime concentrations were evaluated from the weight loss measurements in 1.0 M HCl at 303 - 333 K and the data obtained were fitted to various isotherms using the correlation coefficient (R^2) to determine the best fit. Langmuir isotherm which can be expressed by equation 7, was found to graphically fit the experimental data well:

$$\frac{C_{inh}}{\theta} = \frac{1}{K_{ads}} + C_{inh} \qquad (7)$$

where C_{inh} denotes the concentration of Cefepime in mM, θ denotes the surface coverage and K_{ads} represents the equilibrium constant of adsorption. The plot of C_{inh}/θ vs. C (Figure 2) gave a straight line for the different temperatures suggesting that the adsorption of Cefepime followed Langmuir isotherm.
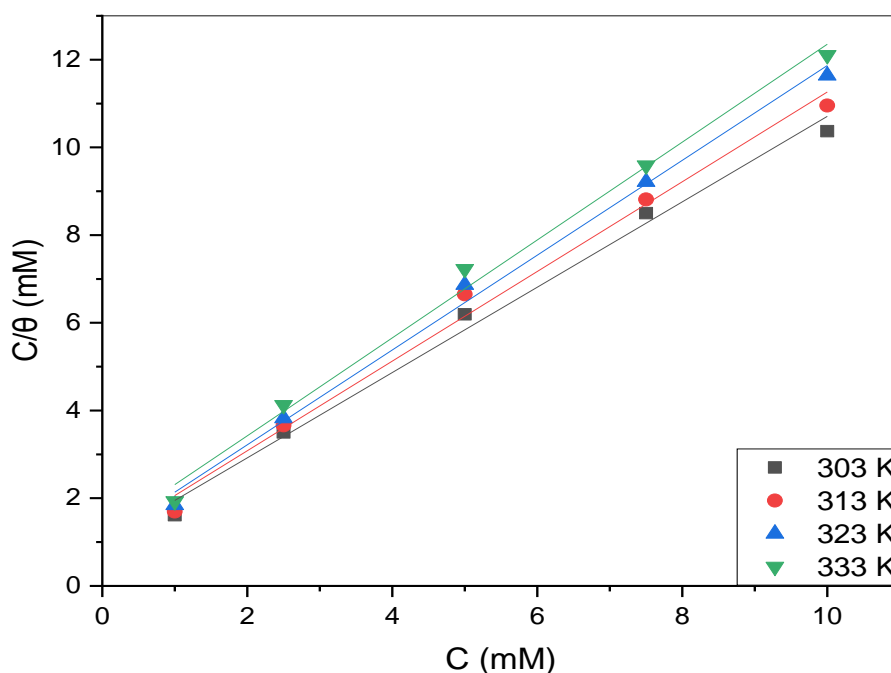

Figure 2: Langmuir adsorption isotherm for adsorption of Cefepime.

The R^2 values of the order of 0.99 with slope in the neighbourhood of unity confirm the suitableness of Langmuir adsorption isotherm model. The K_{ads} evaluated from the intercept of the fitted lines is related to the standard free energy of adsorption (ΔG^o_{ads}) according to the following equation:

$$\Delta G^o_{ads} = -RT \, In \, (55.5 K_{ads}) \qquad (8)$$

where R is the universal constant, T is the absolute temperature and 55.5 is the concentration of water molecules in mol L^{-1}. The various adsorption parameters obtained from the Langmuir isotherm are listed in Table 2.

Table 2: Adsorption parameters obtained from the Langmuir adsorption isotherm plot

T (K)	K_{ads} (mM^{-1})	ΔG_{ads} (kJ/mol)	Slope	R^2
303	31.92	-36.24	0.9731	0.9919
313	19.75	-36.19	1.0224	0.9913
323	13.18	-36.26	1.0810	0.9951
333	10.06	-36.64	1.1158	0.9936

The K_{ads} value has been used to describe the force of adherence that exists between the adsorbate (inhibitor) and adsorbent (steel surface). Large values of K_{ads} indicates enhanced adsorption and therefore improved inhibition efficiency [24]. From the results as seen in Table 2, K_{ads} decreases as temperature increases indicating that the force of adherence of Cefepime to the X80 steel surface decreases with increase in temperature. This behaviour of Cefepime is a combination of both physisorption and chemisorption. The calculated values of ΔG_{ads} gotten are all negative and within the range –36.19 and –36.64 kJ/mol. The negative value suggest that Cefepime is strongly adsorbed on X80 steel surface and ascertains the spontaneity of the adsorption process. The values of ΔG_{ads} are usually used to tag adsorption mechanism as chemisorption, physisorption, or a combination of both adsorption models. Values of ΔG_{ads} in the order of -40 kJ mol^{-1} or more is taken as chemisorption involving charge transfer or sharing from the inhibitors to the metal surface to form a kind of co-ordinate bond while those equal to -20 kJ mol^{-1} or less is interpreted to suggest physisorption involving electrostatic interaction between charged inhibitor molecules [25]. The calculated values of ΔG_{ads} are more negative than –20 kJ mol^{-1} and less negative than –40 kJ mol^{-1}which indicates that Cefepime is adsorbed on X80 steel by both physical and chemical process [26].

3.3. Effect of temperature

The inhibition action of Cefepime was examined at different temperatures (303, 313, 323 and 333 K) using weight measurements. The results presented in Figure 1 (a) shows that increase in temperature causes significant increase in the CR probably due to the desorption of adsorbed Cefepime molecules from the X80 steel surface at elevated temperatures [27]. However, %I_{WL} of the Cefepime decreases with temperature rise as seen in Figure 1 (b). This result indicates physical adsorption of the inhibitor molecules on the steel surface. The effect of temperature can be clearly established using Arrhenius and transition state equations (Eqs. 9 and 10) [28-30].

$$CR = A \exp\left(\frac{-E_a}{RT}\right) \qquad (9)$$

$$CR = \frac{RT}{hN} \exp\left(\frac{\Delta S^*}{R}\right) \exp\left(-\frac{\Delta H^*}{RT}\right) \qquad (10)$$

where, A is the pre-exponential factor, E_a is the activation energy, R is the universal gas constant, T is the absolute temperature, ΔS^* is the entropy of activation, ΔH^* is the enthalpy, N is the Avogadro number, h is the Planck constant. Arrhenius plot of logarithm of CR with reciprocal of absolute temperature (Figure 3a) gives a straight line from which the E_a values were evaluated (Table 3). A plot of log (CR/T) versus 1000/T as shown in Figure 3b gives a straight line with a slope of ($-\Delta H^*/2.303$ R) and an intercept of log (R/Nh + $\Delta S^*/2.303$ R) from which the values of $\Delta H^*$and ΔS^* were deduced and listed in Table 3.

The data in Table 3 clearly shows that E_a values are higher in the presence of Cefepime as compared to in their absence which indicated physisorption mechanism of adsorption that takes place during the initial stage of the interaction between the metal and the inhibitor [31]. Positive values of ΔH^* indicates that the interaction of Cefepime with X80 steel surface is an endothermic process whereas large negative values of ΔS^* indicates that the creation of active complex and dissociation of the complex is the rate determining step [32-34].

Table 3: Kinetic and thermodynamic parameters obtained from Arrhenius and transition state plots

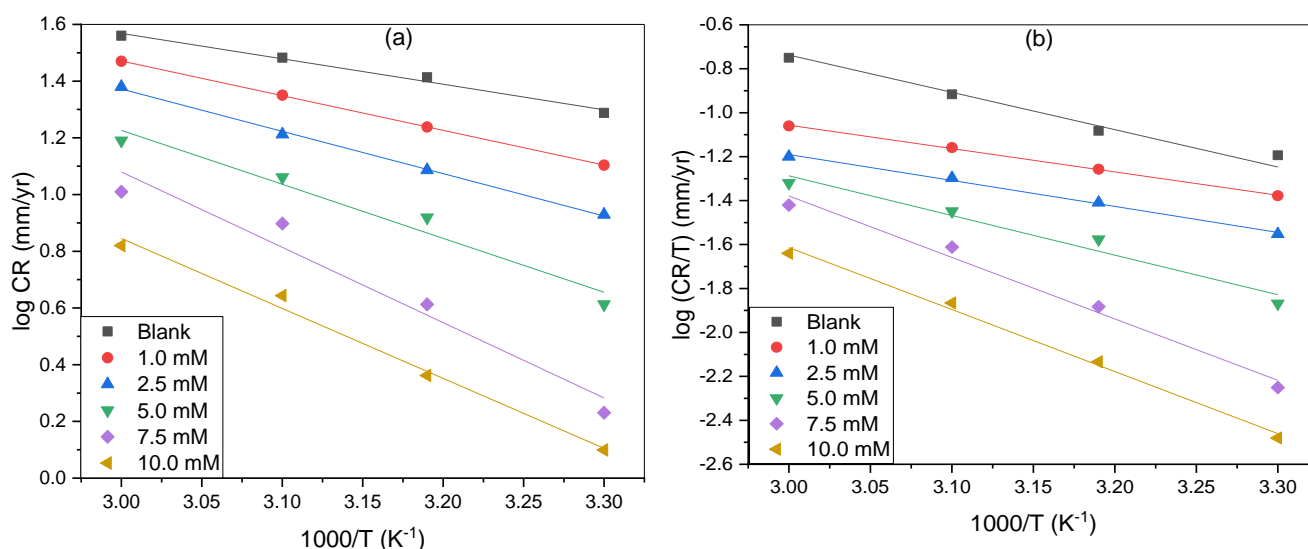| Concentration (mM)	E_a (kJ/mol)	ΔH^*(kJ/mol)	ΔS^* (J/mol/K)
Blank	52.75	50.48	-119.55
1.0	39.06	36.48	-143.87
2.5	36.59	33.72	-147.80
5.0	35.90	33.05	-147.67
7.5	32.18	29.41	-149.80
10.0	30.41	27.76	-151.62

Figure 3: Arrhenius plots (a) of log CR and Transition state plot (b) of log CR/T against 1/T for X80 steel in 1 M HCl and that inhibited by different concentrations of Cefepime

3.4. Electrochemical impedance spectroscopy (EIS) measurement

The EIS is another method that provides valuable information about corrosion inhibition process. The film stability on the metal surface and the kinetics of the electrode processes were also investigated by the EIS measurement. The impedance spectra, presented as Nyquist plots, obtained for corrosion of X80 steel in 1 M HCl in the absence and presence of the Cefepime are presented in Figure 4. It is observed that in all cases the data depicted depressed, capacitive-like semicircles with their centres in the real axis which represents the interaction of the steel surface with the corrosive media. The diameter of the semicircle increases with Cefepime concentration, indicating that the charge transfer process is the main controlling factor of the corrosion of X80 pipeline steel. However, the semicircles in the impedance diagrams are not perfect, which are linked to the frequency dispersion as a result of the roughness and inhomogeneous of steel surface [35-37]. The equivalent circuit model shown in Figure 5 was used to simulates the EIS results. The circuit is made up of solution resistance (R_s) in series with charge transfer resistance (R_{ct}) and double layer capacitance (C_{dl}) simulated through a constant phase element (CPE). The charge transfer resistance values R_{ct} were deduced from the difference in impedance at the lower and higher frequencies [38]. The impedance Z_{CPE} was calculated using Eq. (11):

$$Z_{CPE} = [Y_o\,(j\omega)^n]^{-1} \tag{11}$$

where Y_0 is the magnitude of CPE, j is the imaginary root, ω is angular frequency and n is the exponential term. The values of the double layer capacitance (C_{dl}) was calculated via Eq. (12):

$$C_{dl} = \frac{1}{2\pi f_{max} R_{ct}} \tag{12}$$

where f_{max} is the frequency value at which the imaginary component of the impedance is maximal. The calculated impedance parameters and the inhibition efficiency (%I_{EIS}) of Cefepime are given in Table 4.

Table 4: EIS parameters for X80 steel in 1 M HCl without and with selected concentrations of Cefepime at 303 K

Concentration (mM)	R_s (Ω cm²)	R_{ct} (Ω cm²)	n	Y_o (μ Ω^{-1}s²cm⁻²)	C_{dl} (μFcm⁻²)	%IE$_{EIS}$ (%)
Blank	0.849	68.1	0.895	331.6	94.1	-
5.0	1.395	307.6	0.883	297.4	48.2	77.9
10.0	2.003	998.7	0.913	163.90	20.8	93.2

As seen from Table 4, R_{ct} values increased with an increase in the concentration of the Cefepime reaching a maximum value of 998.7 Ω·cm² at 10 mM concentration of Cefepime while C_{dl} values decreased as Cefepime concentration increases. The increase in R_{ct} values may be due to the formation of adsorbed film of inhibitor molecules on the metal surface. The decrease in C_{dl} may be due to increase in thickness of the electronic double layer [39]. These observations confirm the increasing level of adsorption of Cefepime on the X80 steel surface [40]. The increase in charge transfer resistance and decrease in double layer capacitance as the concentration of the inhibitor increases is ascribed to increasing surface coverage by Cefepime molecules which leads to a corresponding increase in %I_{EIS} with increasing inhibitor concentration.
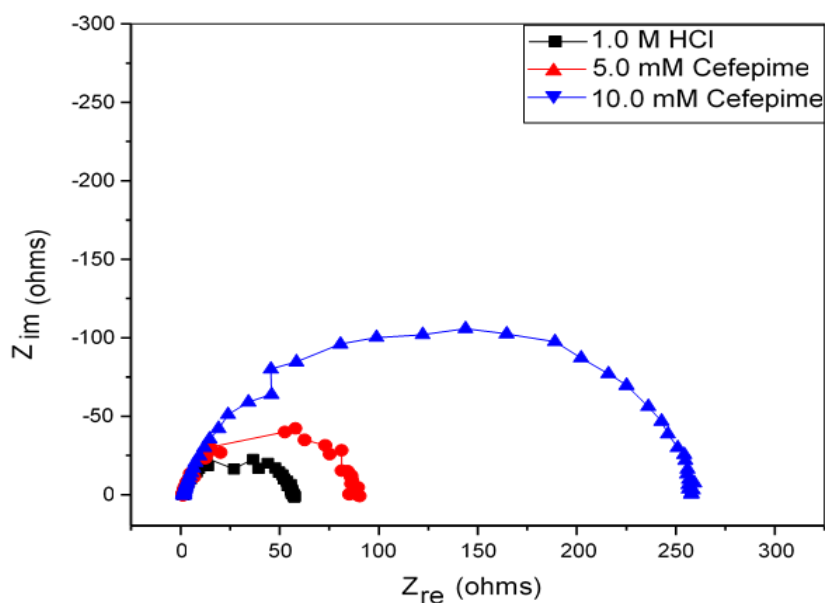

Figure 4: Impedance plots of X80 pipeline steel obtained in 1.0 M HCl in the absence and presence of selected concentrations of Cefepime
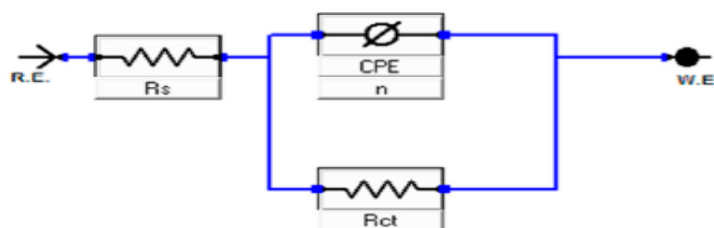

Figure 5: Equivalent Circuit Model.

Iroha and Nnanna, J. Mater. Environ. Sci., 2019, 10 (10), pp. 898-908

904

3.5. Potentiodynamic polarization (PDP) measurement

Polarization curves for X80 steel in 1.0 M HCl solution at selected concentrations of Cefepime at 303 K are shown in the Figure 6. The curves showed that addition of Cefepime to the blank acid solution has mild influence on both anodic metal dissolution process and cathodic H^+ ion reduction half reactions, with anodic influence appearing to be more pronounced. The values of current densities (I_{corr}), corrosion potential (E_{corr}), anodic Tafel slopes (β_a), cathodic Tafel slopes (β_c) and inhibition efficiency as a functions of Cefepime concentration were calculated from the curves and listed in Table 5. The results showed that, as the concentration of Cefepime increased, the values of I_{corr} decreased which indicates the corrosion inhibiting ability of the inhibitor. It is also observed from Table 5 that the maximum change in E_{corr} values is 19.6 mV which is far less than ±85 mV, indicating that Cefepime behave as mixed-type inhibitor but predominantly anodic [41]. The values of βa and βc for the selected concentrations of Cefepime remarkably reduced compared to the blank acid solution confirming the influence of the inhibitor on both the anodic and cathodic reactions thus supporting the assertion that Cefepime is a mixed-type inhibitor. The inhibition efficiency (%I_{PDP}) was observed to increase with increasing Cefepime concentration which clearly shows that the inhibitor molecules are adsorbed on the X80 steel surface.
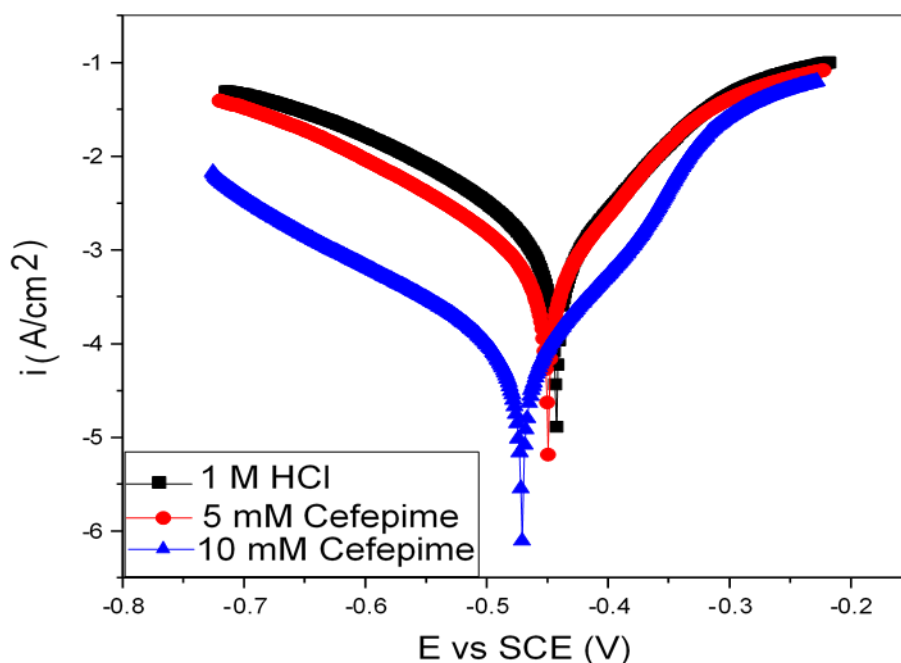

Figure 6: Polarization curves for X80 steel corrosion in the absence and presence of selected concentrations of Cefepime in 1.0 M HCl

Table 5: PDP parameters for X80 pipeline steel corrosion in the absence and presence of selected concentrations of Cefepime in 1.0 M HCl.

Concentration (mM)	I_{corr} (A cm^{-2})	E_{corr} (mV vs SCE)	β_c (mV dec^{-1})	β_a (mV dec^{-1})	IE_{PDP} (%)
Blank	872.1	-392.5	199.7	174.2	
5.0	201.9	-381.3	175.3	132.9	76.8
10.0	69.9	-372.9	157.8	87.9	92.0

3.6. Surface Morphology

The surface morphology of X80 steel in 1.0 M HCl without and with Cefepime was conducted using Scanning electron microscope (SEM). Figure 7(a) shows specimen corroded in 1 M HCl solution without the inhibitor. The surface of the steel in the uninhibited solution is eroded, showing a rough surface with significant amount of micro cracks and pores which creates paths for the acid solution to permeate and corrode the metal. However, the surface of the steel corroded in presence of 10 mM Cefepime, shown in Figure 7(b) is smooth and more compact, with much less micro cracks and pores, which indicates that the metal is highly protected because

of the presence of the inhibitor. These observations confirm that the adsorption of Cefepime molecules on the X80 pipeline steel surface inhibits the corrosion of the metal and reduces surface roughness.
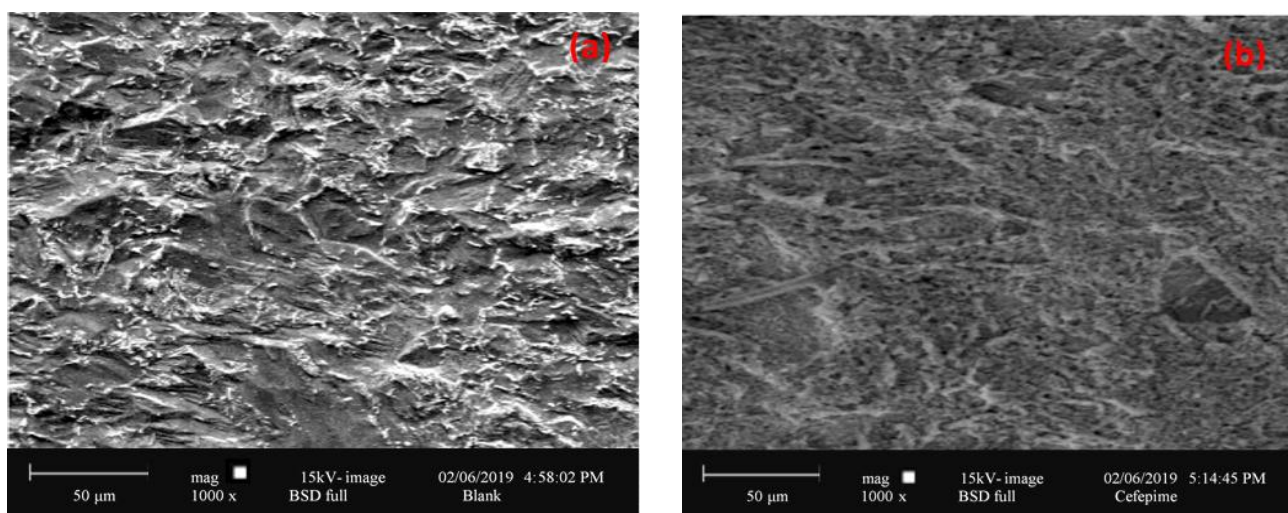

Figure 5: SEM images of X80 pipeline steel surface immersed in 1.0 M HCl (a) without and (b) with 10 mM Cefepime.

Conclusion

Cefepime was investigated as an inhibitor for X80 pipeline steel corrosion in 1.0 M HCl solution. The study revealed that Cefepime is an effective corrosion inhibitor with a better inhibition efficiency at lower temperatures. Cefepime inhibits corrosion by forming a protective film which is physically adsorbed on the X80 steel surface following a Langmuir type of adsorption isotherm. Cefepime acts as mixed type inhibitor but showed the predomination of anodic reaction inhibition. The Inhibition efficiency increased with an increase in the concentration of Cefepime. The SEM images confirm the formation of a protective layer on the X80 steel surface. Cefepime could be an effective alternative corrosion inhibitor for oil-well acidizing practice in the petroleum industry

References

1. L.J. Kalfayan, *Production Enhancement with Acid Stimulation,* ISBN-13: 978-1593703844, Publisher: PennWell Corp.; 2 edition (March 18, 2008)
2. N. Esmaeili, J. Neshati, I. Yavari, Corrosion inhibition of new thiocarbohydrazides on the carbon steel in hydrochloric acid solution, *J. Ind. Eng. Chem.,* 22 (2015) 159–163. https://doi.org/10.1016/j.jiec.2014.07.004
3. M. H. Abd El-Lateef, Experimental and computational investigation on the corrosion inhibition characteristics of mild steel by some novel synthesized imines in hydrochloric acid solutions, *Corros Sci,* 92 (2015) 104–117. https://doi.org/10.1016/j.corsci.2014.11.040
4. M. A. Chidiebere, N. Simeon, D. Njoku, N. B. Iroha, E. E. Oguzie, Y. Li, Experimental study on the inhibitive effect of phytic acid as a corrosion inhibitor for Q235 mild steel in 1 M HCl environment. *WNOFNS*, 15 (2017) 1-19.
5. E. E. Oguzie, G. N. Onuoha, A. I. Onuchukwu, Inhibitory mechanism of mild steel corrosion in 2 M sulphuric acid solution by methylene blue dye, *Mater. Chem. Phys.,* 89 (2005) 305-311. doi:0.016/j.matchemphys.2004.09.004
6. N. B. Iroha, E. E. Oguzie, G. N. Onuoha, A. I. Onuchukwu, Inhibition of Mild Steel Corrosion in Acidic Solution by derivatives of Diphenyl Glyoxal, *16th Int Corros Congress,* (2005) 126-131.
7. D. Daoud, T. Douadi, H. Hamani, S. Chafaa, M. Al-Noaimi, Corrosion inhibition of mild steel by two new S-heterocyclic compounds in 1 M HCl: Experimental and computational study, *Corros Sci*, 94 (2015) 21–37. https://doi.org/10.1016/j.corsci.2015.01.025
8. R. T. Loto, C. A. Loto, A. P. I. Popoola, Corrosion inhibition of thiourea and thiadiazole derivatives: A Review, *J. Mater. Environ. Sci.,* 3 (2012) 885-894.
9. D. G. Ladha, U. J. Naik, N. K. Shah, Investigation of Cumin (Cuminum Cyminum) extract as an eco-friendly green corrosion inhibitor for pure Aluminium in Acid medium, *J. Mater. Environ. Sci.,*4 (2013) 701-708.

10. N. B. Iroha, A. Hamilton-Amachree, Adsorption and Anticorrosion Performance of Ocimum Canum Extract on Mild Steel in Sulphuric Acid Pickling Environment. *Ame. J. Mater. Sci.* 8(2) (2018) 39-44. DOI: 10.5923/j.materials.20180802.03

11. S. A. Umoren, I. B. Obot, E. E. Ebenso, N. O. Obi-Egbedi, Synergistic Inhibition between Naturally Occurring Exudate Gum and Halide Ions on the Corrosion of Mild Steel in Acidic Medium, *Inter. J. Electrochem. Sci.,* 3 (2008) 1029-1043.

12. N.A. Madueke, N.B. Iroha, Protecting aluminium alloy of type AA8011 from acid corrosion using extract from Allamanda cathartica leaves, *Int. J. of Inno Resea in Sci, Eng and Tech*, 7(10) (2018) 10251-10258. DOI: 10.15680/IJIRSET.2018.0710014

13. I. B. Obot, E. E. Ebenso, M. Kabanda, Metronidazole as environmentally safe corrosion inhibitor for mild steel in 0.5 M HCl: experimental and theoretical investigation, *J Environ Chem Eng.,* 1 (2013) 431–439. https://doi.org/10.1016/j.jece.2013.06.007

14. S.K. Shukla, M.A. Quraishi, Cefalexin drug: A new and efficient corrosion inhibitor for mild steel in hydrochloric acid solution, *Mater. Chem. Phys.,* 120 (2010) 142-147. https://doi.org/10.1016/j.matchemphys.2009.10.037

15. A.K. Singh, M.A. Quraishi, Effect of Cefazolin on the corrosion of mild steel in HCl solution, *Corros Sci,* 52 (2010) 152-160. doi:10.1016/j.corsci.2009.08.050

16. P. M. Nouri, M. M. Attar, Experimental and quantum chemical studies on corrosion inhibition performance of fluconazole in hydrochloric acid solution, *Bull. Mater Sci,* 38 (2015) 499–509.

17. D. Yahav, M. Paul, A. Fraser, N. Sarid, L. Leibovici, Efficacy and safety of cefepime: a systematic review and meta-analysis, *Lancet Infect Dis*. 7 (5) (2007) 338–348. DOI: 10.1016/S1473-3099(07)70109-3

18. E. Ituen, O. Akaranta, A. James, Inhibition of Steel Corrosion in Simulated Oilfield Acidizing Medium using Metallic Soap from Local Biomaterial, *Chem. Sci. Int. J.,* 18 (2016) 1–34. doi: 10.11648/j.ogce.20170506.16

19. N.B. Iroha, A. Hamilton-Amachree, Inhibition and adsorption of oil extract of Balanites aegyptiaca seeds on the corrosion of mild steel in hydrochloric acid environment, *World Scientific News,* 126 (2019) 183-197.

20. A.O. James, N.B. Iroha, An Investigation on the Inhibitory Action of Modified Almond Extract on the Corrosion of Q235 Mild Steel in Acid Environment, *IOSR Journal of Applied Chemistry*, 12(2) (2019) 01-10. DOI: 10.9790/5736-1202020110

21. P. Singh, M. A. Quraishi, E. E. Ebenso, Microwave Assisted Green Synthesis of Bis-Phenol Polymer Containing Piperazine as a Corrosion Inhibitor for Mild Steel in 1M HCl, *Int J Electrochem Sci.,* 8 (2013) 10890–10902.

22. N. B. Iroha and A. O. James, Assessment of performance of velvet tamarind-furfural resin as corrosion inhibitor for mild steel in acidic solution *J. Chem Soc. Nigeria,* 43(3) (2018) 510–517

23. M. Özcan, I. Dehri, M. Erbil, Organic sulphur-containing compounds as corrosion inhibitors for mild steel in acidic media: correlation between inhibition efficiency and chemical structure, *Appl. Surf. Sci.*, 236 (2004) 155. https://doi.org/10.1016/j.apsusc.2004.04.017

24. S. O. Ajeigbe, N. Basar, M. A. Hassan, M. Aziz, Optimization of Corrosion Inhibition of Essential Oils of Alpinia Galanga on Mild Steel using Response Surface Methodology, *ARPN J. of Eng. and App. Sci.*, 12(9) (2017) 2763-2771

25. N.B. Iroha, O. Akaranta, A.O. James, Red Onion Skin Extract-formaldehyde Resin as Corrosion Inhibitor for Mild Steel in Hydrochloric Acid Solution, *Int. Resea. J. of Pure & Applied Chemistry*, 6(4) (2015) 174-181. DOI: 10.9734/IRJPAC/2015/9555

26. Y. Ma, F. Han, Z. Li, C. Xia, Acidic-Functionalized Ionic Liquid as Corrosion Inhibitor for 304 Stainless Steel in Aqueous Sulfuric Acid, *ACS Sustain. Chem. Eng.* 4(9) (2016) 5046-5052. https://doi.org/10.1021/acssuschemeng.6b01492

27. Y. El Bakri, L. Guo, E. M. Essassi, Electrochemical, DFT and MD simulation of newly synthesized triazolotriazepine derivatives as corrosion inhibitors for carbon steel in 1 M HCl, *J. Mol. Liq.,* 274 (2019) 759–769. https://doi.org/10.1016/j.molliq.2018.11.048

28. A. Ghazoui, N. Benchat, F. El-Hajjaji, M. Taleb, Z. Rais, R. Saddik, B. Hammouti, The study of the effect of ethyl (6-methyl-3-oxopyridazin-2-yl) acetate on mild steel corrosion in 1M HCl, *J. Alloys Compd*., 693 (2017) 510–517. https://doi.org/10.1016/j.jallcom.2016.09.191

29. M. Mobin, M. Rizvi, Polysaccharide from Plantago as a green corrosion inhibitor for carbon steel in 1M HCl solution, *Carbohydr. Polym.*, 160 (2017) 172–183. doi: 10.1016/j.carbpol.2016.12.056

30. N.B. Iroha, O. Akaranta, A.O. James, (2012), Red onion skin extract-furfural resin as corrosion inhibitor for aluminium in acid medium, *Der Chemica Sinica,* 3(4) (2012) 995-1001.

31. M. A. Quraishi, Sudheer, 2-Amino-3,5-dicarbonitrile-6-thio-pyridines: New and Effective Corrosion Inhibitors for Mild Steel in 1 M HCl, *Ind. Eng. Chem. Res.,* 53(8) 2014 2851–2859. https://doi.org/10.1021/ie401633y

32. N. B. Iroha, N. A. Madueke, Effect of *Triumfetta rhomboidea* Leaves Extract on the Corrosion Resistance of Carbon Steel in Acidic Environment. *Chemical Science International Journal*, 25(2) (2018) 1-9. DOI: 10.9734/CSJI/2018/45807

33. R. Hsissou, S. Abbout, A. Berisha, M. Berradi, M. Assouag, N. Hajjaji, A. Elharfi, Experimental, DFT and molecular dynamics simulation on the inhibition performance of the DGDCBA epoxy polymer against the corrosion of the E24 carbon steel in 1.0 M HCl solution, *J. Mol. Struct*., 1182 (2019) 340–351. https://doi.org/10.1016/j.molstruc.2018.12.030

34. N. El-Aouni, A. Benabida, M. Cherkaoui, A. Elharfi, A New Epoxy Resin Based Organic Molecule as an Effective Inhibitor of Mild Steel Corrosion in a Sulfuric Acid Medium, *J. Chem. Technol. Metall.*, 53(5) 2018 878–890.

35. R.A. Bustamante, G.N. Silve, M.A. Quijano, H.H. Hernandez, Electrochemical study of 2-mercaptoimidazole as a novel corrosion inhibitor for steels, *Electrochim. Acta,* 54 (23) (2009) 5393–5399. https://doi.org/10.1016/j.electacta.2009.04.029

36. S.S.A. Rehim, O.A. Hazzazi, M.A. Amin, K.F. Khaled, On the corrosion inhibition of low carbon steel in concentrated sulphuric acid solutions. Part I: Chemical and electrochemical (AC and DC) studies, *Corrosion Science,* 50(8) (2008) 2258–2271. https://doi.org/10.1016/j.corsci.2008.06.005

37. S. Martinez, M. Metikos-Hukovic, A nonlinear kinetic model introduced for the corrosion inhibitive properties of some organic inhibitors, *J. Appl. Electrochem*., 33 (2003) 1137–1142.

38. S. Tamil Selvi, V. Raman, N. Rajendran, Corrosion inhibition of mild steel by benzotriazole derivatives in acidic medium, *J. Appl. Electrochem*., 33 (2003) 1175-1182.

39. M. G. Hosseini, M. Ehteshamzadeh, T. Shahrabi, Protection of mild steel corrosion with Schiff bases in 0.5 M H_2SO_4 solution, *Electrochem. Acta*., 2007, 52, 3680. https://doi.org/10.1016/j.electacta.2006.10.041

40. A.V. Shanbhag, T.V. Venkatesha, R.A. Prabhu, R. G. Kalkhambkar, G. M. Kulkarni, Corrosion inhibition of mild steel in acidic medium using hydrazide derivatives, *J. Appl. Electrochem*. 38 (2008) 279–287. DOI 10.1007/s10800-007-9436-8

41. M. P. Chakravarthy, K. N. Mohana, C. P. Kumar, Corrosion inhibition effect and adsorption behaviour of nicotinamide derivatives on mild steel in hydrochloric acid solution*Int. J. Indus. Chem*. 5 (2014) 19. DOI:10.1007/s40090-014-0019-3

(2019) ; http://www.jmaterenvironsci.com